JOURNAL OF CATALYSIS 105, 55–64 (1987)

CO Dissociation and C–D Interaction on Ru(001)

L. L. LAUDERBACK* AND W. N. DELGASS

School of Chemical Engineering, Purdue University, West Lafayette, Indiana 47907

Received June 24, 1986; revised November 20, 1986

SIMS and temperature-programmed oxidation show that CO dissociates on Ru(001) at 520 K. SIMS studies show that carbon, but not oxygen, accumulates on the surface. Surface carbon begins conversion to graphite at about 600 K and diffuses into the bulk at temperatures above 800 K. Interaction of deuterium with carbon deposited by CO dissociation increases the D_2 thermal desorption peak temperature by more than 100 K and produces an $RuCD^+$ peak in the SIMS spectrum. The correspondence of the temperature dependence of the $RuCD^+$ signal with the D_2 thermal desorption, the narrowness of the D_2 desorption peak, and the absence of $RuCD_2^+$ or $RuCD_3^+$ peaks indicate formation of a well-defined C–D species on the surface.

INTRODUCTION

Ruthenium is one of the most active Fischer–Tropsch synthesis catalysts and has a unique propensity to yield high-molecular-weight straight chain paraffins (*1–3*). A number of recent studies suggest that synthesis of hydrocarbons over ruthenium involves the dissociation of CO followed by hydrogenation of the resulting carbon and polymerization of various hydrocarbon intermediates. Infrared studies (*3–5*), for example, show that while molecular CO is the dominant surface species, absorption bands due to C–H stretch modes are also observed which indicate the presence of hydrocarbon intermediates. Tamaru *et al.* (*5*) report that the C–H bands of hydrocarbons on Ru catalysts correspond to liquid aliphatic hydrocarbons; a finding consistent with the high selectivity of ruthenium for straight chain paraffins.

The dissociation of CO on Ru has also been examined. Goodman and White (*6*) observed the dissociation of CO and the associated buildup of carbidic carbon on Ru(110) during exposure to 10 Torr CO. They also report the transformation of that carbon to graphite upon heating above ~600 K. Papagno *et al.* (*7*) similarly observed dissociation of CO and formation of carbidic carbon on Ru(101) following a 90-min CO exposure at $\sim 7 \times 10^{-3}$ Pa and transformation of the carbidic carbon to graphite after heating to 970 K for 2 min. More recently, Tamaru and co-workers (*8*) studied the interaction of CO with Ru(001) and the stepped Ru(1,1,10) surfaces. On the stepped Ru(1,1,10) surface they observed a β-CO state at 580 K in the thermal desorption spectrum following CO exposures up to ~60 L at 501 K. This state was shown to correspond to dissociated CO. Transformation of carbidic surface carbon to graphite was also observed on the Ru(1,1,10) surface after heating to 840 K. No β-CO was found, however, on Ru(001) following the same treatment. In a separate study that utilized higher CO pressures and exposures, Tamaru *et al.* (*9*) did observe CO dissociation on Ru(001) following a $\sim 10^7$-L CO exposure at a pressure of 4.2 Pa. The rate of CO dissociation under the same conditions was much faster, however, on the stepped Ru(1,1,10) surface and contribution from the edges of the crystal could not be ruled out in the Ru(001) experi-

* Present address: Department of Chemical Engineering, University of Colorado, Boulder, CO 80309.

0021-9517/87 $3.00

ments. Negligible CO dissociation on Ru(001) after small to moderate exposures has also been reported previously (*10–13*). In the most extreme of these attempts, exposures of more than 1000 L CO at 490 K did not produce β-CO on subsequent thermal desorption (*11*). This rules out dissociation which leaves high amounts of carbon and oxygen on the surface but does not rule out CO disproportionation to produce surface carbon and desorbed CO_2, since small amounts of carbon could not be resolved from the Ru signals in either Auger or X-ray photoelectron spectra (*11*).

Several studies have shown that carbidic carbon deposited by CO dissociation on Ru catalysts can be hydrogenated rapidly, while graphitic carbon is much less reactive (*14, 15*). The carbidic phase is thus thought to be the active form involved in hydrocarbon synthesis, while graphite is associated with catalyst deactivation. Transient and isotopic labeling studies show, furthermore, that the rate limiting step in hydrocarbon synthesis over ruthenium involves the hydrogenation of surface CH_x intermediates (*5, 16–18*).

Less certain is the chemical identity of the hydrocarbon intermediates and the mechanism of chain growth. Biloen and Sachtler (*19*) suggest that the active hydrocarbon intermediates consist of a mixture of CH, CH_2, and CH_3 species in addition to polymeric hydrocarbons. Bell *et al.* (*20, 21*) report evidence for the presence of CH_2 species and suggest that hydrocarbon chain growth occurs by successive addition of such methylene intermediates. Direct evidence for the existence of most of these hydrocarbon synthesis intermediates on Ru is sparse, however. The only reports to date that provide direct observation of such intermediates come from the HREELS studies of Barteau *et al.* (*22, 23*) which demonstrate the formation of CH species on Ru(001) when surface carbon formed by dissociation or hydrogenolysis of ethylene, or by electron-stimulated dissociation of CO, was exposed to hydrogen and heated to 370 K under ultrahigh vacuum (UHV) conditions.

In this report we examine the dissociation of CO on Ru(001), the chemical nature of the carbon deposited by CO dissociation, and the interaction of that carbon with deuterium. Evidence of CO disproportionation on Ru(001) is obtained directly from SIMS and temperature-programmed oxidation (TPO) measurements. The initial chemical state of the carbon deposited by dissociation of CO and the transformation of that carbon to graphite upon heating is also characterized by TPO. The nature of the interaction of carbon deposited by CO dissociation with deuterium is examined using deuterium thermal desorption spectroscopy (TDS) and SIMS. The utility of SIMS for directly probing the nature of the C–D interaction is demonstrated.

EXPERIMENTAL

All experiments were carried out in ion-pumped, stainless-steel, ultrahigh vacuum chamber with a base pressure of about 1×10^{-10} Torr. In SIMS experiments, primary Ar^+ ions were generated by a Riber CI 50-ion gun and secondary ions were detected with a Riber Q156 quadrupole mass spectrometer equipped with a 45° sector energy prefilter. The mass spectrometer is also equipped with an ionization filament for residual gas analysis and thermal desorption measurements. All experiments were performed with a 5-keV Ar^+ ions impinging on the sample surface at a 45° polar angle measured form the surface normal. The primary ion current density was 5×10^{-8} A/cm^2.

The Ru single crystal was oriented by Laue X-ray backscattering to within 1° of the Ru(001) plane, cut by a diamond saw, and mechanically polished. After being etched in hot aqua regia for about 15 min, the crystal was spot welded to two tantalum heating wires which were connected to two stainless-steel electrodes on a sample manipulator. The temperature was monitored by a Pt/Pt–10% Rh thermocouple which was spot welded to the back of the crystal.

In this configuration, temperatures up to 1700 K could be routinely achieved. The surface cleaning procedure, which was similar to that used by Madey *et al.* (*10*) involved many heating and cooling cycles up to 1600 K in 5×10^{-7} Torr of oxygen followed by heating in vacuum 2–5 times to 1700 K to remove surface oxygen. Surface cleanliness was verified by AES and SIMS.

RESULTS AND DISCUSSION

Dissociation of CO on Ru(001)

We illustrate first the disproportionation of CO on Ru(001) and the utility of SIMS for distinguishing between molecular and dissociative CO adsorption by comparing SIMS spectra of Ru(001) surfaces saturated with molecular $C^{18}O$ at 320 K (exposure = 9.0 L) and following a 480-L ^{13}CO exposure (5×10^{-7} Torr) at 520 K. These spectra are presented in Fig. 1A and B, respectively. In the Ru^+ and Ru_2^+ mass regions, both spectra are characteristic of the Ru isotope distribution which runs from 96–104 amu and allows easy identification of Ru- and Ru_2-containing clusters. The appearance of the cationized $C^{18}O$ ions, $RuC^{18}O^+$, in Fig. 1A directly reflects the presence of molecular $C^{18}O$ following the 9.0-L $C^{18}O$ dose at 320 K. This assignment follows from an earlier study (*24*) which showed by isotope mixing experiments that CO groups present in the $RuCO^+$ ions form directly from CO molecules that eject intact. The small yields of RuC^+ and $Ru^{18}O^+$ in Fig. 1A are derived by fragmentation of some $C^{18}O$ molecules during ejection and are not indicative of dissociated $C^{18}O$ since they disappear together with $RuC^{18}O^+$ and $Ru_2C^{18}O^+$ when the $C^{18}O$ layer is desorbed by heating. In contrast to $C^{18}O$ adsorption at 320 K, we do not expect to see irreversible adsorption of molecular ^{13}CO at 520 K since thermal desorption measurements (*10, 24*) show that molecular CO desorbs rapidly at temperatures above ~425 K. The absence of any molecular ^{13}CO following the 480-L ^{13}CO exposure

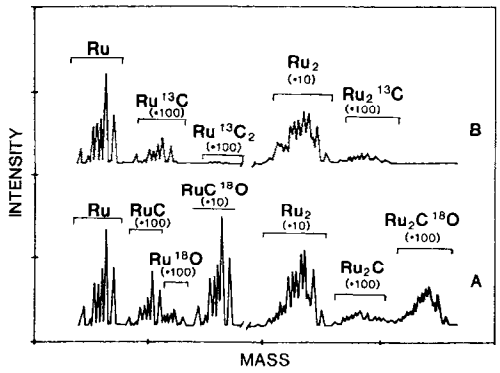

FIG. 1. Positive ion SIMS spectra following (A) 9.0 L $C^{18}O$ at 320 K, (B) 480-L ^{13}CO exposure at 520 K. (From Ref. 32; reprinted with permission from the ACS Symposium Series. Copyright 1985 American Chemical Society.)

at 520 K is confirmed by the absence of $Ru^{13}CO^+$ and $Ru_2^{13}CO^+$ ions in Fig. 1B. We therefore interpret the appearance of the $Ru^{13}C^+$ and $Ru_2^{13}C^+$ ions in Fig. 1B as a direct indication of ^{13}C deposition via ^{13}CO dissociation. Also of interest is the absence of RuO^+ and Ru_2O^+ ions in spectrum 1B. Since these ions are known to be characteristic of adsorbed oxygen atoms (*25*), this result suggests that unlike carbon, oxygen does not accumulate on the surface during dissociation of ^{13}CO. It therefore appears that oxygen formed during dissociation of ^{13}CO at 520 K either reacts with molecular ^{13}CO and desorbs as $^{13}CO_2$ or diffuses into the bulk. We note that the absence of surface oxygen is consistent with the results of Tamaru *et al.* (*8*) who also report an absence of surface oxygen and β-CO following exposure of Ru(001) to a 90-L CO dose at ~500 K. Tamaru and co-workers (*8*) did not, however, analyze their Ru(001) surface for carbon following the 90-L CO dose. We believe that the present work is the first example of CO dissociation on Ru(001) under UHV conditions. While lack of observation of CO disproportionation in previous studies can be traced to the absence of a definitive test for the presence of surface carbon, assignment of the activity found in this work to the close-packed sur-

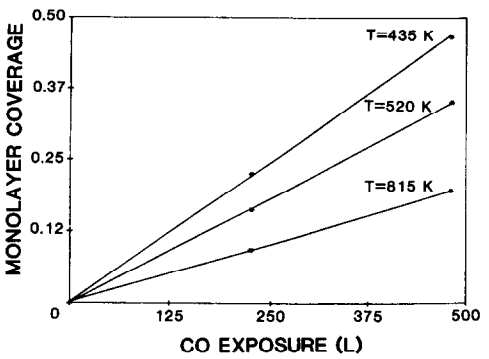

FIG. 2. Carbon coverage as a function of ^{13}CO exposure at 435, 520, and 815 K.

face must be accepted with caution. Our methods of crystal cleaning and annealing are identical to those reported in the literature to give well-ordered surfaces. Furthermore, CO and O_2 thermal desorption spectra from our crystal are in excellent agreement with reported results (*10, 26*). Nevertheless, known high rates of CO dissociation on steps (*8*) and the lack of direct observation of surface order in our experiments make it impossible to rule out an influence of defect sites.

The amount of carbon deposited on the surface as a function of ^{13}CO exposure and temperature was determined by measuring the amount of ^{13}CO evolved during temperature-programmed titration of the deposited carbon with oxygen. This procedure involved exposing the sample to the desired dose of ^{13}CO ($P = 5 \times 10^{-7}$ Torr) at the desired temperature. The sample was then cooled in vacuum to 340 K and exposed to 6.0 L oxygen. The ^{13}CO mass spectrometer signal was then monitored while increasing the sample temperature at a linear rate of 6 K/sec until the evolution of ^{13}CO ceased at ~750 K. In all cases the amount of ^{13}C deposited was low enough such that all of the surface carbon could be removed in one titration. The complete removal of ^{13}C following this procedure was confirmed by SIMS. Contributions due to formation of $^{13}CO_2$ were neglected since the rate of $^{13}CO_2$ formation was determined to be approximately 100 times lower than the rate of CO formation. Figure 2 shows the dependence of the amount of carbon deposited as a function of ^{13}CO exposure and temperature. At each of the three temperatures investigated, the rate of ^{13}C deposition appears to be nearly constant for exposures up to the maximum investigated, ~480 L. The rate of carbon deposition is also seen to decrease with increasing temperature, which we interpret as being caused by a decrease in the ^{13}CO coverage with increasing temperature. The reaction probabilities for deposition of ^{13}C per incident ^{13}CO molecule as computed from the slopes of the curves in Fig. 2 are 4.9×10^{-4}, 3.7×10^{-4}, and 2.1×10^{-4} at 435, 520, and 815 K, respectively.

Effect of Temperature on the Chemical Nature of Surface Carbon

We examine next the influence of temperature on the chemical nature of the deposited carbon using temperature-programmed oxidation (TPO). In these measurements, a carbon layer was deposited by exposing the sample to a 480-L ^{13}CO dose at 520 K. The surface was then annealed by heating in vacuum at a rate of 6 K/sec to the desired temperature and then cooled to 340 K. The TPO spectra were obtained by exposing the cooled sample to 6.0 L O_2 and heating at a linear rate of 6 K/sec while monitoring the ^{13}CO mass spectrometer signal. As mentioned above, CO_2 accounts for less than 1% of the oxidation so the ^{13}CO signal accounts for essentially all of the carbon removed. The TPO spectra for various annealing temperatures are presented in Fig. 3. In the case of the 323 K spectrum, we note that the sample was cooled to 323 K following carbon deposition and was not subsequently annealed prior to oxygen adsorption. The 323 K TPO spectrum exhibits a broad peak centered at ~540 K and a second peak at ~615 K. As the annealing temperature increases to 663 K, the high temperature peak at 615 K disappears and is replaced by a high tempera-

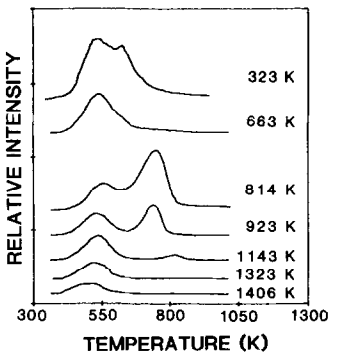

FIG. 3. Temperature-programmed oxidation spectra following a 480-L ^{13}CO dose at 520 K, annealing to the temperatures indicated, and cooling to 340 K.

ture shoulder. An annealing temperature of 814 K produces a new high temperature peak at ~740 K, while the intensity of the low temperature peak is reduced significantly. Further increases in temperature above 814 K cause the high temperature peak to decay rapidly and to shift toward higher temperature while the low temperature peak at 540 K decays more slowly and remains at an essentially constant temperature. The appearance of the new high temperature peaks at ~740 K and the concurrent decline in intensity of the 540 K TPO peak as the annealing temperature increases above 663 K is analogous to that observed in our earlier studies of carbon adlayers formed by dissociation of ethylene on Ru(001) (*27*). In that study, the low temperature TPO peak was shown to be associated with the oxidation of a reactive, low density (presumably carbidic) form of carbon while the high temperature peak was indicative of the formation of less reactive, high density graphitic islands. In the present case, we therefore interpret the decline in intensity of the 540 K TPO peak and concurrent appearance of the new high temperature peak at ~740 K as the result of conversion of carbidic carbon to the graphite phase upon annealing above 663 K. Similar conversions of carbidic carbon to the graphite phase during thermal treatment have also been reported by Goodman and White (*6*) on Ru(110), Papagno *et al.* (*7*) on Ru(101), and by Tamaru *et al.* (*9*) on Ru(1,1,10). The decline in the amount of ^{13}CO evolved with increasing temperatures above 814 K is also similar to that observed when carbon is deposited by dissociation of ethylene on Ru(001) (*27*) and is indicative of diffusion of carbon into the bulk. This is seen more clearly in Fig. 4 which presents a plot of the amount of ^{13}CO evolved in TPO vs annealing temperature.

Also of interest is the observation that as the annealing temperature increases above 814 K the intensity of the high temperature peak associated with the graphite phase declines much more rapidly than the 540 K TPO peak. In fact, the 1323 and 1406 K TPO spectra in Fig. 3 show that the high temperature TPO peak completely disappears before 540 K TPO peak. This behavior was also observed in ethylene-derived carbon layers in Ru(001) (*27*) and suggests that a minimum surface coverage of carbon is required for the formation of graphite. This is consistent with the work of Kelley and Goodman (*28*) who also find a minimum carbon coverage necessary to produce graphite on Ru(110) and with the findings of Tamaru *et al.* (*9*) who observed that higher carbon coverage enhances the formation of graphite on Ru(1,1,10).

Finally, we note the appearance of the 615 K TPO peak in the 323 K spectrum and

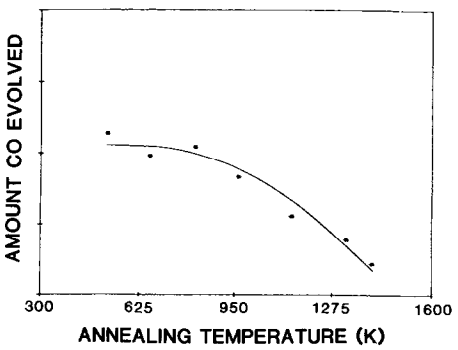

FIG. 4. Relative amount of ^{13}CO evolved as a function of annealing temperature in the temperature-programmed oxidation spectra of Fig. 3.

its disappearance upon annealing to 663 K. This behavior is also similar to that of ethylene-derived carbon on Ru(001) (*27*). A detailed analysis of the TPO spectra for that system suggested that the broad low temperature peak results from first-order desorption of CO derived from nonmobile carbon and oxygen atoms located on adjacent sites, while the high temperature peak appearing in the 323 K TPO spectrum is associated with the onset of carbon and oxygen mobility and results from surface-diffusion-controlled, second-order desorption of CO. Loss of the high temperature (~615 K) second-order peak after annealing to 663 K corresponded with the onset of graphite formation which began slowly at roughly ~600 K. In view of the analogous behavior of the TPO spectra obtained in this study to those of our earlier study (*27*), we interpret the disappearance of the 615 K peak in Fig. 3 after annealing to 663 K as a sensitive indication of the onset of graphite formation. The strong sensitivity of the high temperature second-order ~615 K peak to the initial stage of the carbidic to graphite transformation apparent in both studies suggests that even the small aggregates of carbon that form during the initial step of graphite formation have a much lower reactivity toward oxygen than isolated carbon atoms.

Interaction of Deuterium with Surface Carbon

Previous studies of coadsorbed H_2 and CO indicate no positive interaction between molecularly adsorbed hydrogen and carbon monoxide (*29, 30*). We also find that CO either displaces preadsorbed H_2 or blocks post adsorption of H_2, and that thermal desorption peak temperatures are not perturbed by coadsorption. Furthermore, SIMS spectra of coadsorbed D_2/CO adlayers are the same as those of adlayers containing CO only and thus confirm lack of interaction of the molecularly adsorbed species.

The interaction of deuterium with carbon deposited by disproportionation of CO is more interesting. The influence of various amounts of surface carbon deposited by dissociation of ^{13}CO on the deuterium thermal desorption spectrum is shown in Fig. 5. The spectrum for desorption of deuterium from the clean surface is also shown for comparison. The measurements were performed by first exposing the sample to the desired dose of ^{13}CO at 520 K. The sample was then cooled to 425 K and exposed to 720 L D_2. Following the deuterium exposure, the sample was heated at a rate of approximately 65 K/sec by application of a constant heating voltage while monitoring the D_2 mass spectrometer signal. We note that since molecular CO blocks adsorption of deuterium, deuterium exposures were carried out at 425 K instead of room temperature to prevent irreversible adsorption of CO from the background gas during the long deuterium exposures. The results seen in Fig. 5 show that the presence of surface carbon produces a new D_2 thermal desorption peak appearing at a significantly higher temperature than that for desorption from the clean surface. The peak maximum of the new desorption state appears at ~540 K and is essentially independent of ^{13}CO exposure, and hence carbon coverage, although the amount of deuterium that adsorbs increases significantly with carbon

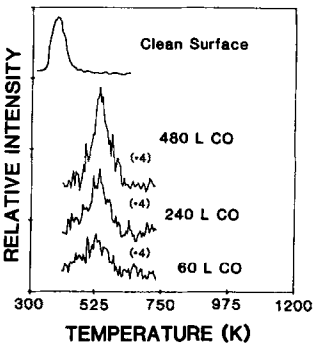

FIG. 5. D_2 thermal desorption spectra from clean Ru(001) and from surfaces preexposed at 520 K to the ^{13}CO doses indicated. (From Ref. 32; reprinted with permission from the ACS Symposium Series. Copyright 1985 American Chemical Society.)

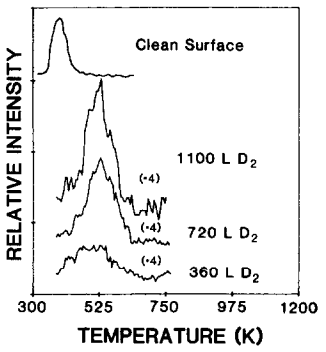

FIG. 6. D_2 thermal desorption spectra for the indicated D_2 exposures at 425 K following a 480-L ^{13}CO exposure at 520 K.

coverage. We also note that the desorption peak is relatively narrow and symmetric for all ^{13}CO exposures. The appearance of the new high temperature desorption state on the carbon-containing surfaces shows that the presence of surface carbon creates new deuterium bonding sites that have significantly higher heat of adsorption than those available on the clean surface. The relatively narrow desorption peaks and the invariance of the peak maximum with carbon and deuterium coverage indicates that the presence of surface carbon creates only a single new type of bonding state that has a specific bonding energy as opposed to a distribution of new states. This suggests the possibility that the new state might correspond to the formation of a specific molecular CD complex of well-defined C–D bond energy. This possibility is explored in more detail below using SIMS, but first the deuterium TDS spectra as a function of deuterium coverage at constant carbon coverage are discussed.

Figure 6 presents a series of deuterium thermal desorption spectra for various deuterium exposures at 425 K following a 480-L ^{13}CO exposure at 520 K. These results also show the presence of a single desorption peak at ~530 K for all deuterium exposures. The observed invariance of the peak positions with deuterium coverage is indicative of a first-order desorption process and suggests that the rate limiting desorption step involves the breaking of deuterium bonds associated with the high bond energy sites created by the surface carbon. The independence of the peak positions with coverage additionally suggests that the heat of adsorption of deuterium does not vary with deuterium coverage. This supports the notion that the presence of surface carbon creates only a single type of adsorption site since if a distribution of adsorption sites having different bonding energies were created, one would expect the higher bond energy sites to fill first and the desorption curve to shift toward lower temperatures as the coverage increased. The weak signals obtained in these studies make quantitative analysis of the desorption peaks difficult. Estimates from the Redhead analysis (*31*), assuming first-order desorption with a preexponential factor of 10^{13} sec^{-1}, give a value of ~30 kcal/g-mole for the activation energy of C–D bond breaking. The analysis of Chan *et al.* (*32*) suggests that both the activation energy and preexponential factor have lower values.

SIMS

We next use SIMS to examine the nature of the strong C–D interaction indicated by the thermal desorption measurements. The positive ion SIMS spectrum of a surface exposed to 480 L ^{13}CO at 520 K followed by a 720-L D_2 exposure at 425 K is shown in Fig. 7A. For purpose of comparison, we

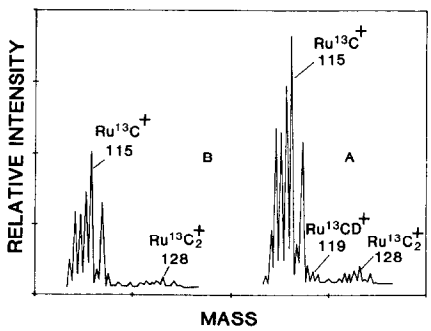

FIG. 7. Positive ion SIMS spectra in the $RuC–RuC_2$ mass region following (A) a 480-L ^{13}CO dose at 520 K followed by a 720-L D_2 dose at 425 K, (B) a 480-L ^{13}CO dose at 520 K.

show in Fig. 7B the SIMS spectrum of a surface exposed only to 480 L ^{13}CO at 520 K. Both spectra were recorded at 425 K using an ion current density of 10^{-7} A/cm^2. In these experiments, we are primarily interested in the formation of $RuC_xD_y^+$ ions which might reflect the presence of a deutero-carbon complex and, therefore, only the RuC–RuC_2 mass region was scanned to minimize ion damage. The appearance of $Ru^{13}C^+$ and $Ru^{13}C_2^+$ ions in both spectra shown in Fig. 7 indicates the presence of surface carbon formed by disproportionation of ^{13}CO. Of particular interest however, is the appearance of the peak at *m/e* = 119 in spectrum A that does not appear in spectrum B. This peak corresponds to the *m/e* value for an $Ru^{13}CD^+$ ion containing the heaviest isotope (*m/e* = 104) of Ru. $RuCD^+$ peaks corresponding to lighter Ru isotopes are masked by isotopic interference with the $Ru^{13}C$ peaks. In support of the assignment of the *m/e* = 119 peak to an $RuCD^+$ ion we note that when ^{12}CO instead of ^{13}CO is dissociated prior to the 720-L D_2 exposure, the resulting SIMS spectrum shows no peak at *m/e* = 119. The appearance of the *m/e* = 119 peak in Fig. 7 thus specifically requires the presence of both ^{13}C and D as expected for the formation of an $RuCD^+$ ion.

To obtain additional support for this assignment and to probe the relationship of the *m/e* = 119 peak to the strong C–D interaction indicated by the thermal desorption spectra, we examine the temperature dependence of the *m/e* = 119 ion intensity. In this experiment, the intensity of the *m/e* = 119 peak was measured after heating the sample to successively higher temperatures and cooling to 425 K. Figure 8 compares the resulting temperature dependence of the *m/e* = 119 peak with the deuterium thermal desorption spectrum for the case involving a 480-L ^{13}CO exposure at 520 K followed by a 720-L D_2 exposure at 425 K. The result shows that the *m/e* = 119 peak intensity decreases to essentially zero over the temperature region of the deuterium thermal desorption peak. We interpret this result, in combination with the specificity of the *m/e* = 119 peak to ^{13}C and D, as a strong indication that the *m/e* = 119 peak corresponds to an $RuCD^+$ ion that directly reflects the strong C–D interaction indicated by the thermal desorption spectrum.

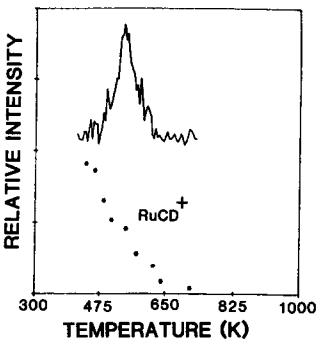

FIG. 8. Comparison of the temperature dependence of the $RuCD^+$ ion intensity obtained after heating the pretreated surface to successively higher temperatures and cooling to 425 K to the D_2 thermal desorption spectrum obtained after a pretreatment consisting of 480 L ^{13}CO at 520 K followed by a 720-L D_2 exposure at 425 K.

In considering the nature of the surface species responsible for emission of the $RuCD^+$ ion and the strong C–D interaction, we note that molecular surface species are often emitted intact during ion bombardment and appear directly in the SIMS spectrum as the ionized and/or cationized parent molecule (*24, 33–38*). The appearance of the cationized CD molecule, $RuCD^+$, in the SIMS spectrum thus suggests that the strong C–D interaction might correspond to the formation of a surface CD molecule. This is furthermore consistent with the formation of a deuterium bonding state of specific bond energy, as indicated by the TDS spectra discussed above, since the distribution of C–D bond energies among molecular CD species is likely to be rather narrow. Another possibility however, is that the $RuCD^+$ ion might be formed by a mechanism involving recombination of C and D atoms that are emitted independently and subsequently recombine. Both theory (*35,*

38–40) and experiment (*27, 34, 35, 37, 41*) indicate that this mechanism will dominate the formation of $RuCD^+$ if C and D are located in close proximity to each other without being associated as a bound molecular CD entity. This latter constraint follows from the fact that bound molecular entities tend to eject intact, as discussed above. We, therefore, expect that $RuCD^+$ ions formed by such a recombination mechanism would most likely be indicative of deuterium bonded to high energy metal sites created by a through-metal type electronic interaction with carbon, since this would require close proximity between ^{13}C and D atoms but not a strong C–D bond. The formation of such high energy metal sites is, however, inconsistent with a single bonding state of specific bond energy at all carbon and deuterium coverages, as indicated by the TDS spectra, since through-metal interactions would be likely to produce a distribution of metal–D bond energies due to the nonuniform local distribution of carbon and the variation of the influence of carbon on metal sites with distance from the carbon atoms. Thus, we conclude that the TDS and SIMS data, when considered together, are most consistent with the idea that the strong C–D interaction is caused by the formation of molecular CD entities on the surface. This conclusion is supported by the HREELS data of Barteau *et al.* (*22, 23*) which show the formation of surface CH species on Ru(001) when surface carbon is exposed to hydrogen and heated to 370 K under UHV conditions. Surface CH species are also reported by Weinberg *et al.* after decomposition of C_2H_4 or C_2H_2 on Ru(001) (*42, 43*). It is of interest to note that we do not observe any $RuCD_2^+$ ions which would indicate the presence of surface CD_2 species. This is also consistent with the HREELS data of Barteau *et al.* (*22, 23*) which similarly show no evidence for surface CH_2 species following exposure of surface carbon to hydrogen. It thus appears that deuteration of the CD species to form CD_2 is either too slow to be observed under UHV conditions or that CD_2 species are too reactive to be present on the surface in observable concentrations.

CONCLUSIONS

SIMS and TPO studies show that ^{13}CO dissociates on Ru(001) under UHV conditions resulting in the deposition of surface carbon. SIMS studies also reveal that unlike carbon, oxygen does not accumulate on the surface during dissociation of ^{13}CO, suggesting that oxygen leaves the surface as $^{13}CO_2$ by reaction with ^{13}CO or diffuses into the bulk. TPO measurements indicate that the carbon deposited by dissociation of ^{13}CO undergoes a carbide to graphite phase transition upon heating above ~600 K and begins to diffuse into the bulk when the surface is heated above ~800 K. TPO measurements also suggest that a minimum carbon coverage is required for the formation of graphite. Deuterium TDS studies of the interaction of deuterium with carbon deposited by dissociation of ^{13}CO at 520 K show that the surface carbon creates a new deuterium bonding site that has a much higher bond energy than those available on the clean surface. SIMS studies of the same C–D interaction reveal emission of an $RuCD^+$ ion, the intensity of which has the same temperature dependence as the population of the new high energy deuterium state seen in the TDS spectra. The appearance of the $RuCD^+$ ion in the SIMS spectrum thus directly reflects the strong ^{13}C–D interaction indicated by the TDS spectra and illustrates the utility of SIMS for probing surface chemistry. We interpret the SIMS and deuterium TDS results as being consistent with the formation of a surface molecular CD entity.

ACKNOWLEDGMENTS

We are grateful for support of this work by NSF Grants ChE 78-08728, CPE 7911597, and DMR 77-23798 and by the Amoco Oil Company and The Exxon Education Foundation.

REFERENCES

1. Vannice, M. A., *J. Catal.* **37,** 462 (1975).
2. Vannice, M. A., *Catal. Rev.-Sci. Eng.* **14,** 153 (1976).
3. Ekerdt, J. G., and Bell, A. T., *J. Catal.* **58,** 170 (1979).
4. King, D. L., *J. Catal.* **61,** 77 (1980).
5. Kobori, Y., Yamasaki, H., Naito, S., Onishi, T., and Tamaru, K., *J. Chem. Soc. Faraday Trans. I* **78,** 1473 (1982).
6. Goodman, D. W., and White, J. M., *Surf. Sci.* **90,** 201 (1979).
7. Papagno, L., Caputi, L. S., Ciccacci, F., and Mariani, C., *Surf. Sci.* **128,** L209 (1983).
8. Shincho, E., Egawa, C., Naito, S., and Tamaru, K., *Surf. Sci.* **149,** 1 (1985).
9. Shincho, E., Egawa, C., Naito, S., and Tamaru, K., *Surf. Sci.* **155,** 153 (1985).
10. Madey, T. E., and Menzel, D., *Jpn. J. Appl. Phys., Suppl. 2, part 2,* 229 (1974).
11. Fuggle, J. C., Madey, T. E., Steinkilberg, M., and Menzel, D., *Surf. Sci.* **52,** 521 (1975).
12. Fuggle, J. C., Umbach, E., Feulner, P., and Menzel, D., *Surf. Sci.* **64,** 69 (1977).
13. Thomas, G. E., and Weinberg, W. H., *J. Chem. Phys.* **70,** 954 (1979).
14. Rabo, J. A., Risch, A. P., and Poutsma, M. L., *J. Catal.* **53,** 295 (1978).
15. Low, G. G., and Bell, A. T., *J. Catal.* **57,** 397 (1979).
16. Araki, M., and Ponec, V., *J. Catal.* **44,** 439 (1976).
17. Biloen, P., Helle, J. N., van den Berg, F. G. A., and Sachtler, W. M. H., *J. Catal.* **81,** 450 (1983).
18. Winslow, P., and Bell, A. T., *J. Catal.* **86,** 158 (1984).
19. Biloen, P., and Sachtler, W. M. H., *Adv. Catal.* **30,** 165 (1981).
20. Ekerdt, J. G., and Bell, A. T., *J. Catal.* **62,** 19 (1980).
21. Bell, A. T., *Catal. Rev.-Sci. Eng.* **23,** 203 (1981).
22. Barteau, M. A., Broughton, J. Q., and Menzel, D., *Appl. Surf. Sci.* **19,** 92 (1984).
23. Barteau, M. A., Feulner, P., Stengl, R., Broughton, J. Q., and Menzel, D., *J. Catal.* **94,** 51 (1985).
24. Lauderback, L. L., and Delgass, W. N., *Phys. Rev. B* **26,** 5258 (1982).
25. Lauderback, L. L., and Delgass, W. N., unpublished results.
26. Madey, T. E., Engelhardt, H. A., and Menzel, D., *Surf. Sci.* **48,** 304 (1975).
27. Lauderback, L. L., and Delgass, W. N., *Surf. Sci.* **172,** 715 (1986).
28. Kelley, R. D., and Goodman, D. W., *Surf. Sci.* **123,** L743 (1982).
29. Peebles, D. E., Schreifels, J. A., and White, J. M., *Surf. Sci.* **116,** 117 (1982).
30. Fisher, G. B., Madey, T. E., and Yates, J. T., Jr., *J. Vac. Sci. Technol.* **15,** 543 (1978).
31. Redhead, P. A., *Vacuum* **12,** 203 (1962).
32. Chan, C.-M., Aris, R., and Weinberg, W. H., *Appl. Surf. Sci.* **1,** 360 (1978).
33. Benninghoven, A., *J. Vac. Sci. Technol.* **3,** 451 (1985).
34. Delgass, W. N., Lauderback, L. L., and Taylor, D. G., Springer Series in Chemical Physics, Vol. 20, p. 51, Springer-Verlag, Berlin, 1982.
35. Garrison, B. J., and Winograd, N., *Science* **216,** 805 (1982).
36. Lauderback, L. L., and Delgass, W. N., "Catalytic Materials: Relationship between Structure and Reactivity" (T. E. Whyte, Jr., R. A. Della Betta, E. G. Derouane, and R. T. Baker, Eds.), ACS Symposium Series, Vol. 248, p. 21. *Amer. Chem. Soc.*, Washington, D.C., 1984.
37. Winograd, N., "Desorption Mass Spectrometry" (P. A. Lyon, Ed.), ACS Symposium Series, Vol. 291, p. 82. *Amer. Chem. Soc.*, Washington, D.C., 1985.
38. Garrison, B. J., "Desorption Mass Spectrometry" (P. A. Lyon, Ed.), ACS Symposium Series, Vol. 291, p. 43. *Amer. Chem. Soc.*, Washington, D.C., 1985.
39. Garrison, B. J., Winograd, N., and Harrison, D. E., *Phys. Rev. B* **18,** 6000 (1978).
40. Winograd, N., Harrison, D. E., and Garrison, B. J., *Surf. Sci.* **78,** 767 (1978).
41. Lauderback, L. L., and Delgass, W. N., "Solid State Chemistry in Catalysis" (R. K. Grasselli and J. F. Brazdil, Eds.), ACS Symposium Series, Vol. 279, p. 339. *Amer. Chem. Soc.*, Washington, D.C., 1985.
42. Hills, M. M., Parmeter, J. E., Mullins, C. B., and Weinberg, W. H., *J. Amer. Chem. Soc.* **108,** 3554 (1986).
43. Parmeter, J. E., Hills, M. M., and Weinberg, W. H., *J. Amer. Chem. Soc.* **108,** 3563 (1986).